Electronic Supplementary Information

Concise Nanotherapeutic Modality for Cancer Involving Graphene Oxide Dots in Conjunction with Ascorbic Acid

Chun-Yan Shih,[a, b, c] Pei-Ting Wang,[a, b, c] Wei-Pang Chung,[b, d] Wen-Hsiu Wang,[e] I-Ting Chiang,[b] Wu-Chou Su,[b, d] Wei-Lun Huang,[b, e] * and Hsisheng Teng [a, b, c] *

a. Department of Chemical Engineering, National Cheng Kung University, Tainan 70101, Taiwan.

b. Center of Applied Nanomedicine, National Cheng Kung University, Tainan 70101, Taiwan.

c. Hierarchical Green-Energy Materials (Hi-GEM) Research Center, National Cheng Kung University, Tainan 70101, Taiwan

d. Department of Oncology, National Cheng Kung University Hospital, College of Medicine, National Cheng Kung University, Tainan 70101, Taiwan.

e. Department of Medical Laboratory Science and Biotechnology, College of Medicine, National Cheng Kung University, Tainan 70101, Taiwan.

*Corresponding Authors

Wei-Lun Huang

E-mail: allenhuang@mail.ncku.edu.tw

Hsisheng Teng

E-mail: hteng@mail.ncku.edu.tw

Table of Contents

1. Chemical structures of H_2Asc derivatives
2. Chemical properties of NGODs
3. H_2O_2 production in the presence of high concentrations of H_2Asc
4. EPR for TEMPO-OH standard
5. HPLC spectrum of NGODs-H_2Asc solutions
6. Biocompatibility of NGODs
7. Quantification of GSH depletion
8. Electronic band levels of NGODs determination
9. Determination of cell death mechanisms by Annexin V/PI assay
10. Determination of mitochondrial damage by TMRE assay

1. Chemical structures of H_2Asc derivatives

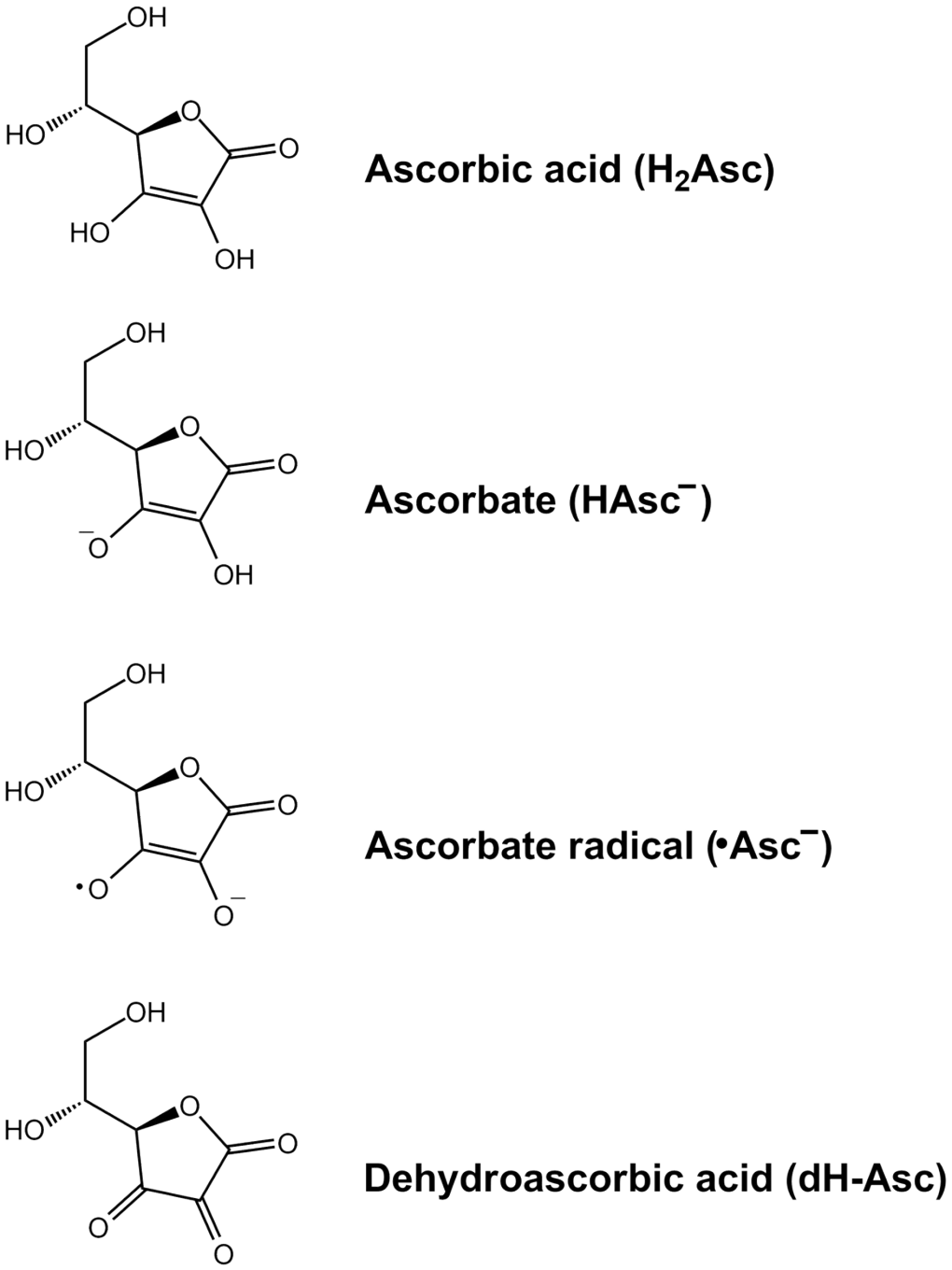

Fig. S1. Chemical structures of H_2Asc derivatives.

2. Chemical properties of NGODs

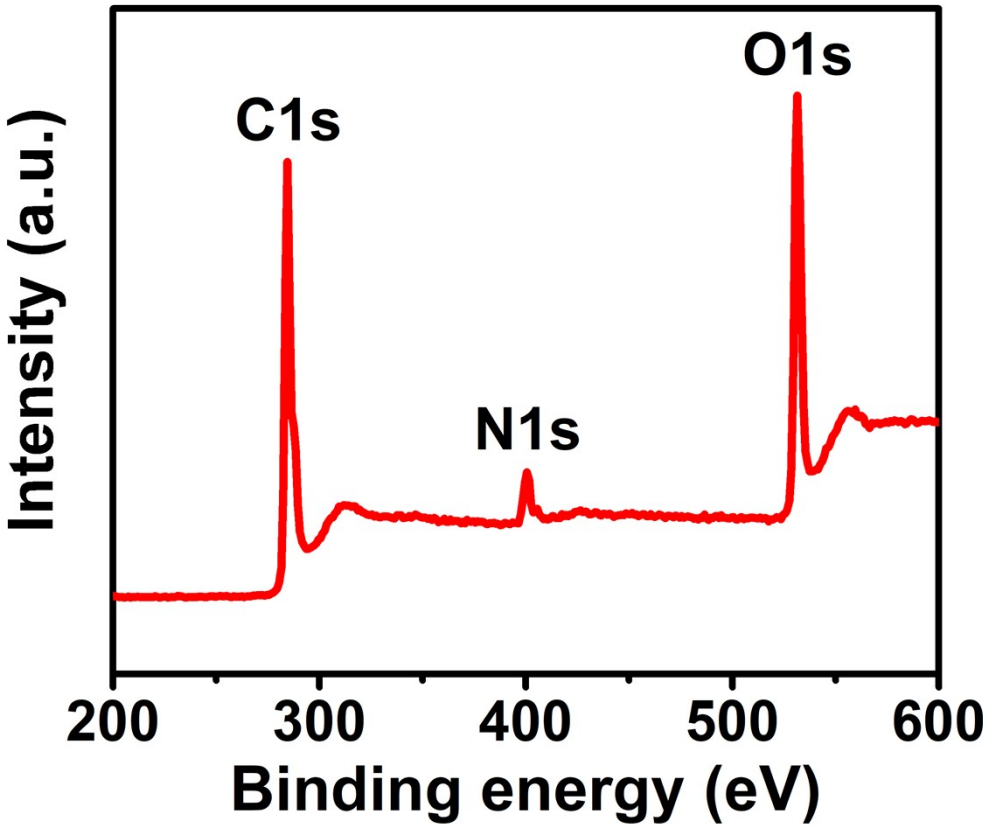

Fig. S2. Full-range XPS spectrum of NGODs.

Table S1. The (O 1s)/(C 1s) and (N 1s)/(C 1s) atomic ratios were derived from the full-range XPS spectrum (Fig. S1), the composition of carbon bonding was derived from the C 1s XPS spectrum (Fig. 1d) , and the composition of nitrogen functionality was derived from the N 1s XPS spectrum (Fig. 1c).

	Atomic ratio (%)	Carbon bonding composition (%)				
	O 1s / C 1s	C-C	C-N	C-O	C=O	O-C=O
NGODs	38.8	68.3	3.93	10.8	15.2	1.76

	Atomic ratio (%)	Nitrogen functionality composition (% of C 1s)			
	N 1s / C 1s	Pyridine	Pyrrolic	Graphitic	Oxidized
NGODs	7.96	0.43	2.24	4.22	1.06

3. H_2O_2 production in the presence of high concentrations of H_2Asc

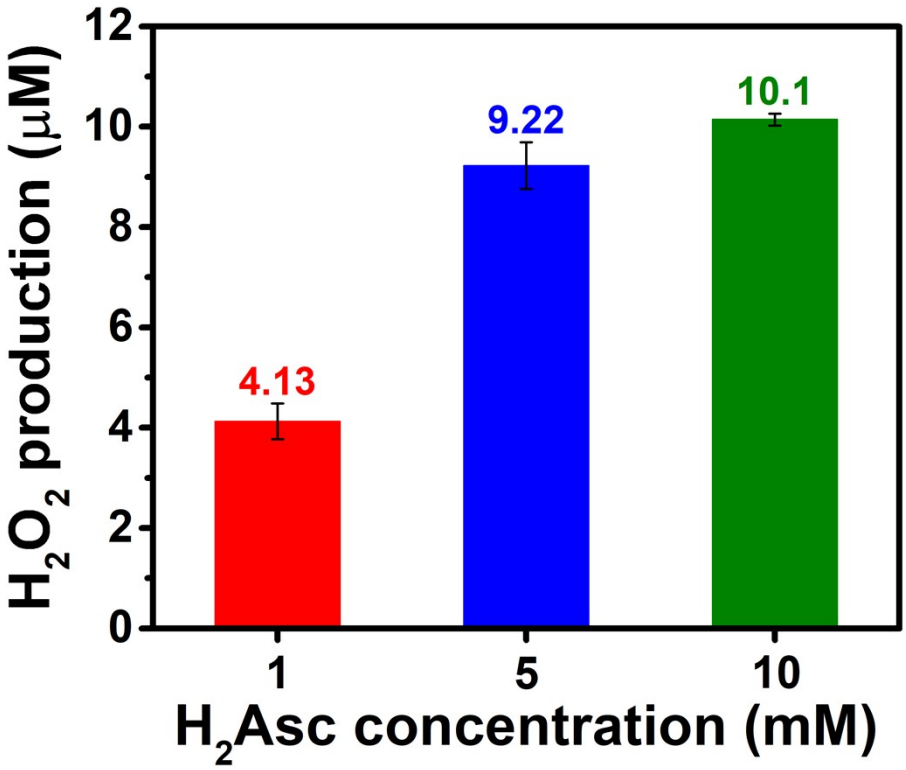

Fig. S3. H_2O_2 prodution over different concentrations of H_2Asc concentrations (1, 5, and 10 mM) in aqueous solution.

4. EPR for TEMPO-OH standard

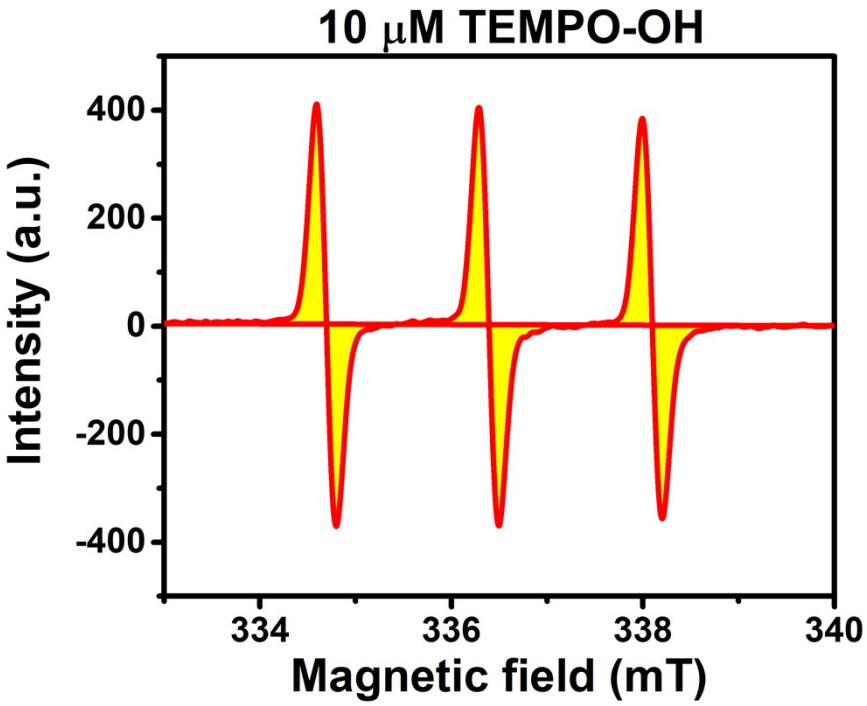

Fig. S4. EPR spectrum of 10 μM TEMPO-OH (note: yellow area under curve integrated as a standard).

5. HPLC spectrum of NGODs-H_2Asc solutions

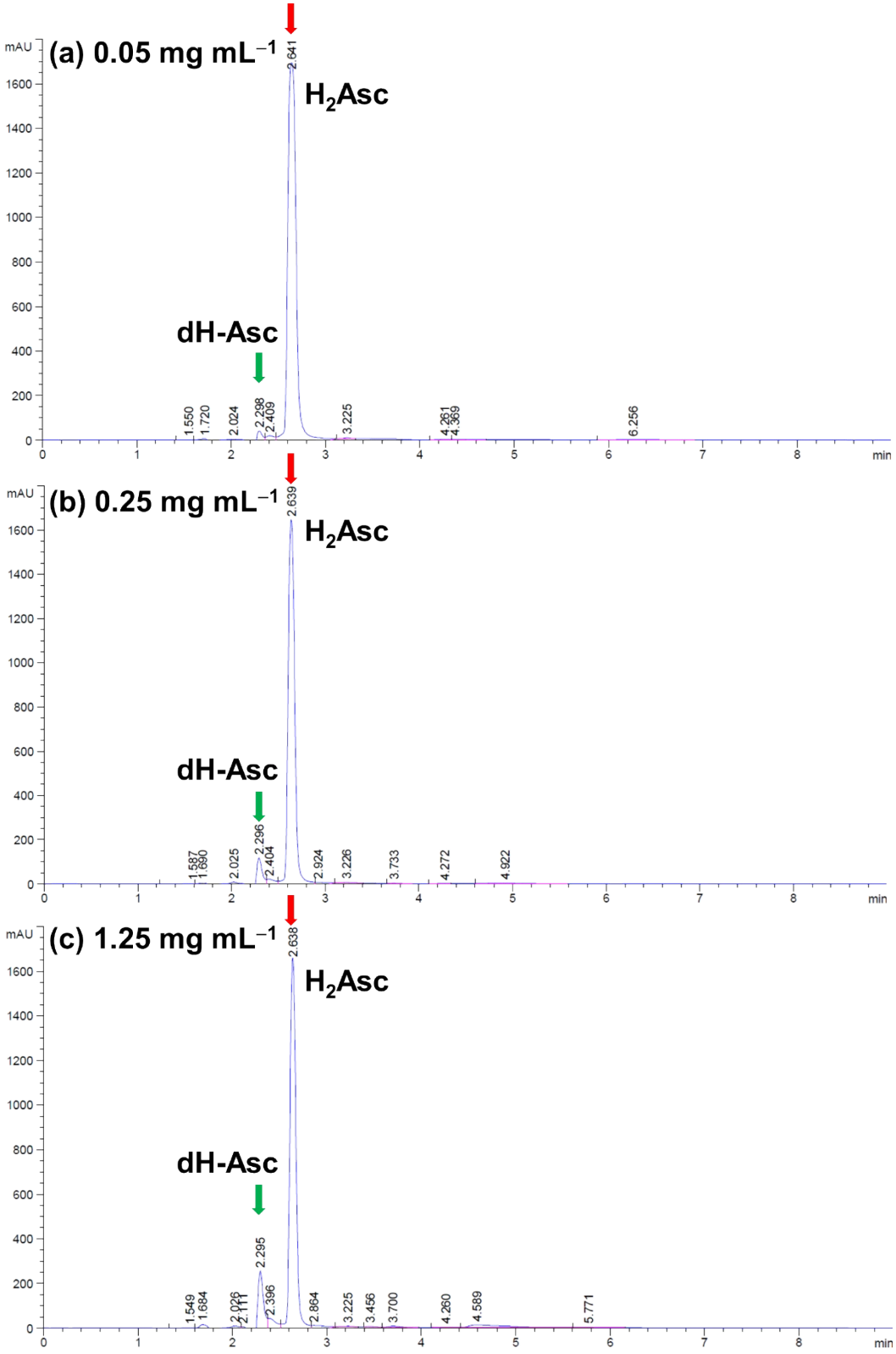

Fig. S5. HPLC spectra of H_2Asc solutions (5 mM) after incubation with different concentrations of NGODs for 4 h: (a) 0.05 mg mL^{-1}; (b) 0.25 mg mL^{-1}; and (c) 1.25 mg mL^{-1} .

6. Biocompatibility of NGODs

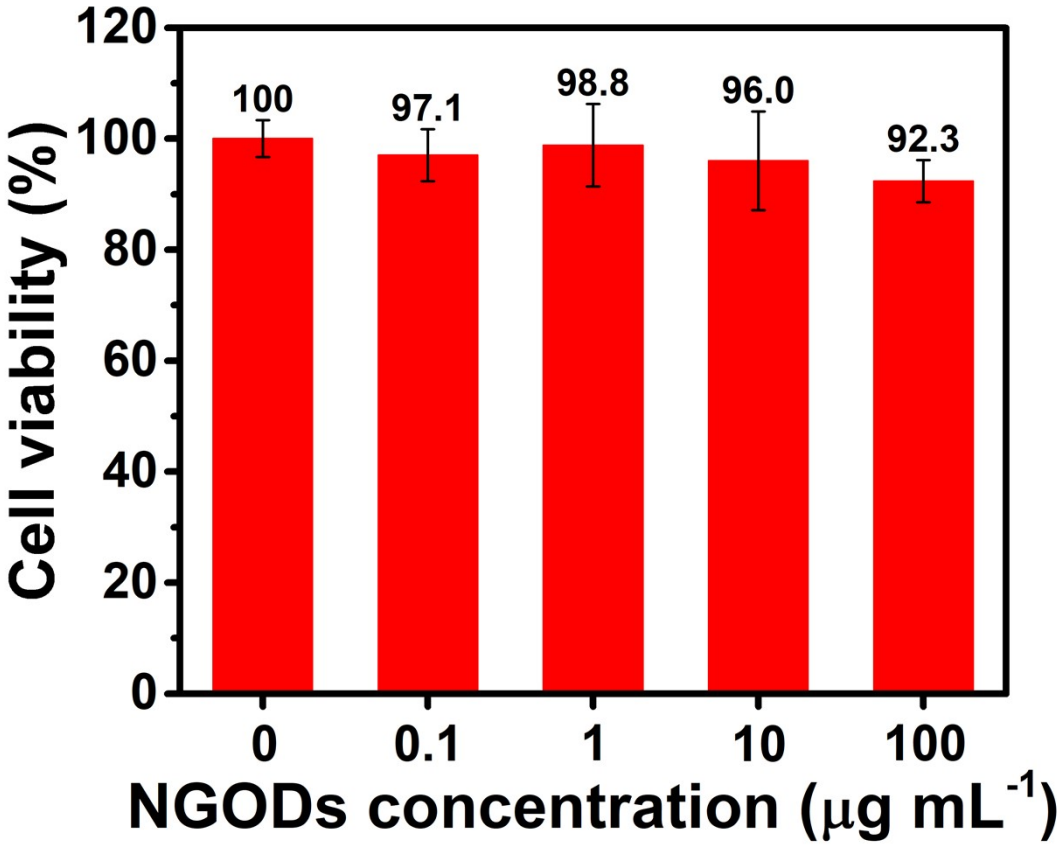

Fig. S6. Biocompatibility of NGODs with L929 cell in accordance with ISO 10993-5 standards where cell viability as a function of NGODs concentrations was determined via MTT assay at 24 h after NGODs treatment (note: plot presents mean values and error bars represent standard error).

7. Quantification of GSH depletion

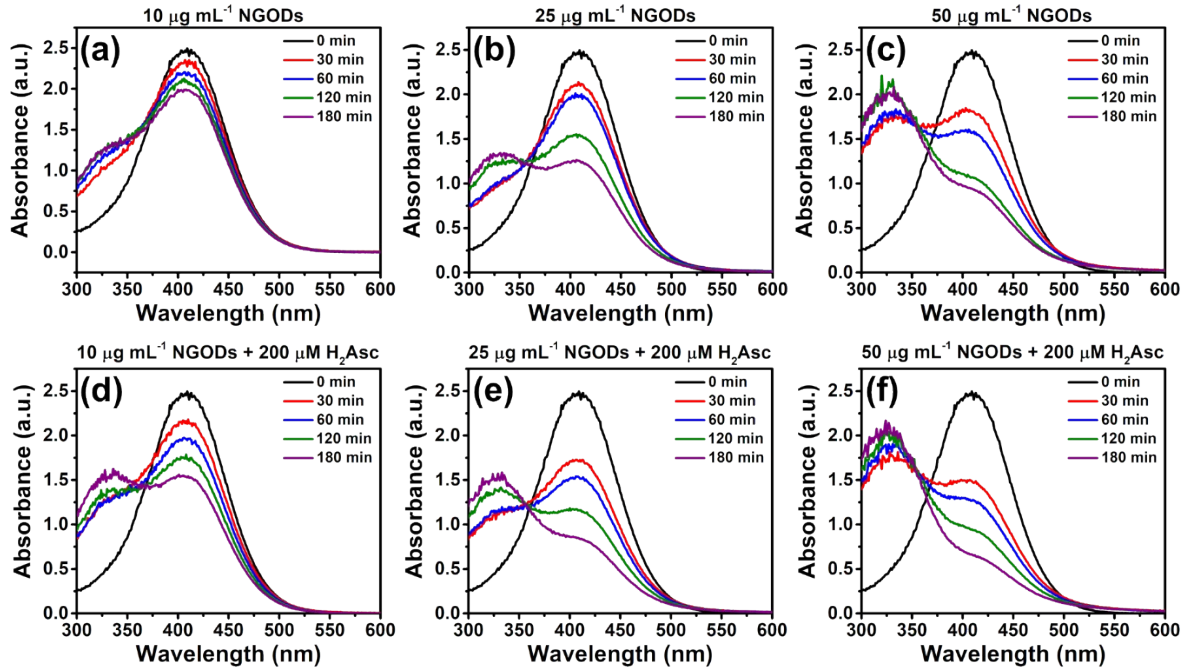

Fig. S7. Absorption spectra indicating GSH depletion over time (with respective GSH and DTNB concentrations of 1 mM and 0.5 mM): (a) NGOD–GSH–DTNB solution with 10 μg mL^{-1} NGODs; (b) NGOD–GSH–DTNB solution with 25 μg mL^{-1} NGODs; (c) NGOD–GSH–DTNB solution with 50 μg mL^{-1} NGODs; (d) NGOD–H_2Asc–GSH–DTNB solution with 10 μg mL^{-1} NGODs; e) NGOD–H_2Asc–GSH–DTNB solution with 25 μg mL^{-1} NGODs; f) NGOD–H_2Asc–GSH–DTNB solution with 50 μg mL^{-1} NGODs and 200 μM H_2Asc.

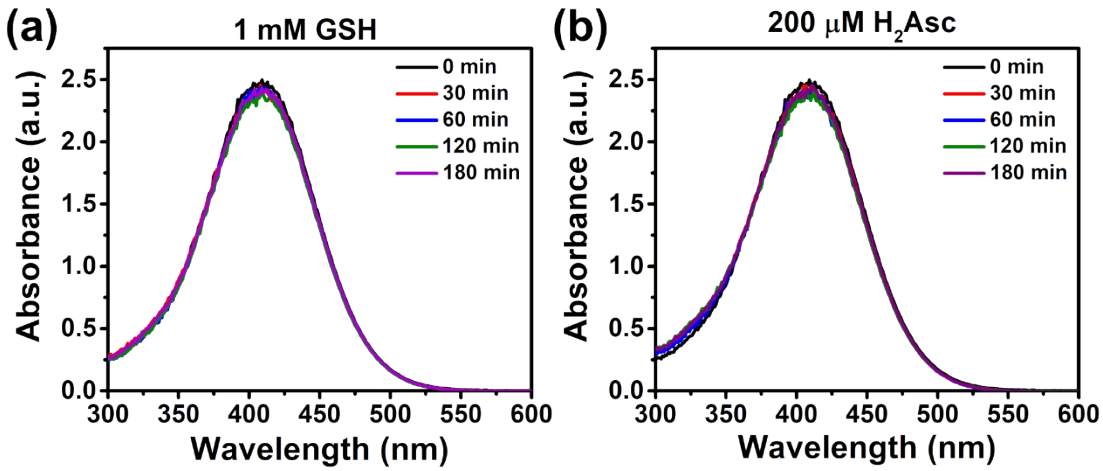

Fig. S8 Variations in absorption spectra indicating GSH depletion over time (with respective GSH, DTNB, H_2Asc concentrations of 1 mM, 0.5 mM, and 200 μM): (a) GSH–DTNB solution; (b) H_2Asc–GSH–DTNB solution.

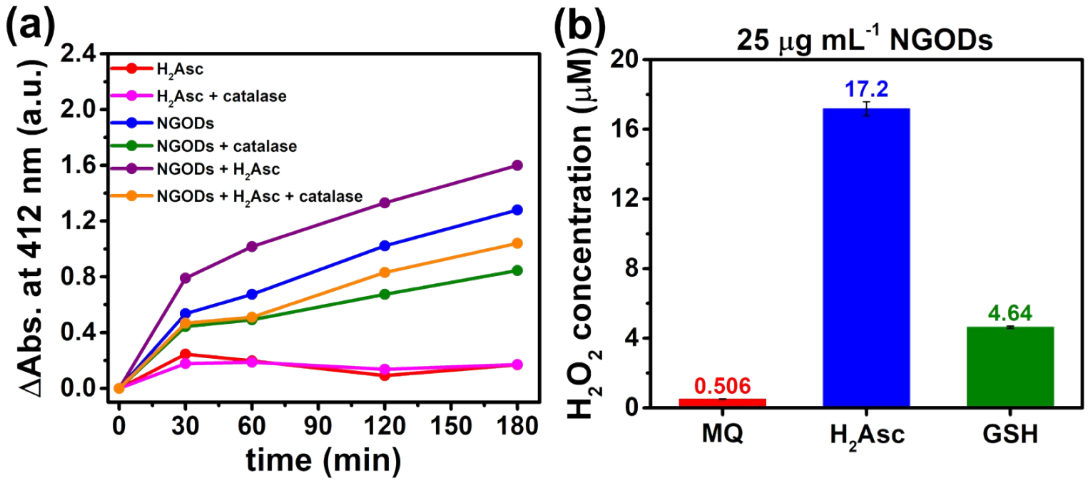

Fig. S9 (a) Magnitude of decrease in TNB at 412 nm over time indicating GSH depletion with 1.5 U mL^{-1} of catalase (where 1 U corresponds to the amount of enzyme that would decompose 1 μmol H_2O_2 per minute at pH 7.0 and 25 °C) and without catalase (with respective concentrations of H_2Asc and NGODs of 200 μM and 25 μg mL^{-1}) ; (b) H_2O_2 production over NGODs in ultra-pure water (MQ), H_2Asc, or GSH solution (with respective concentrations of NGODs, H_2Asc, and GSH of 25 μg mL^{-1}, 200 μM, and 1 mM).

8. Electronic band levels of NGODs determination

For electrochemical analysis, NGOD working electrodes were prepared by drop-casting NGODs aqueous solutions on fluorine-doped Tin Oxide (FTO) conducting glass substrates. NGOD electrodes electrochemical analysis was carried out in 0.5 M HNO_3 solution with a Pt wire counter and an Ag/AgCl (3 M KCl) reference electrodes. Linear scan voltammetric analysis was used to determine the VBM and CBM at a scanning rate 0.5 mV s^{-1}. Fig. S10a,b show the anodic and cathodic scanning results indicating VBM and CBM values of 1.13 and −1.50 V (vs. Ag/AgCl), respectively. The calculated bandgap energy was 2.63 V based on this scan. Alternating current (AC) impedance spectroscopy (BioLogic VMP3, Germany) was performed to determine Fermi level (E_F) potentials at a frequency of 45.409 kHz, based on the Mott-Schotty equation, in which a linear relationship between $1/C^2$ and applied potential can be found. The Fermi level of NGODs was obtained from the intercept of the extrapolated straight line on the x-coordinate in Fig. S10c. Cyclic voltammetric analysis was conducted to determine the H_2Asc oxidation potential. We subjected bare FTO conducting glass as a working electrode with a Pt wire counter and an Ag/AgCl (3 M KCl) reference in 0.5 M HNO_3 solution containing 500 μM H_2Asc at scanning rate 10 mV s^{-1}. Fig. S10d presents a cyclic voltammogram of H_2Asc (500 μM) indicating an H_2Asc oxidation potential of roughly 0.63 V (vs. Ag/AgCl). Fig. S10e presents energy-level diagrams of NGODs. The bandgap between the VBM and CBM (2.63 eV in width) encompassed the energy levels for H_2Asc oxidation and O_2 reduction, indicating that NGODs are capible of catalyzing these two reactions under illumination.

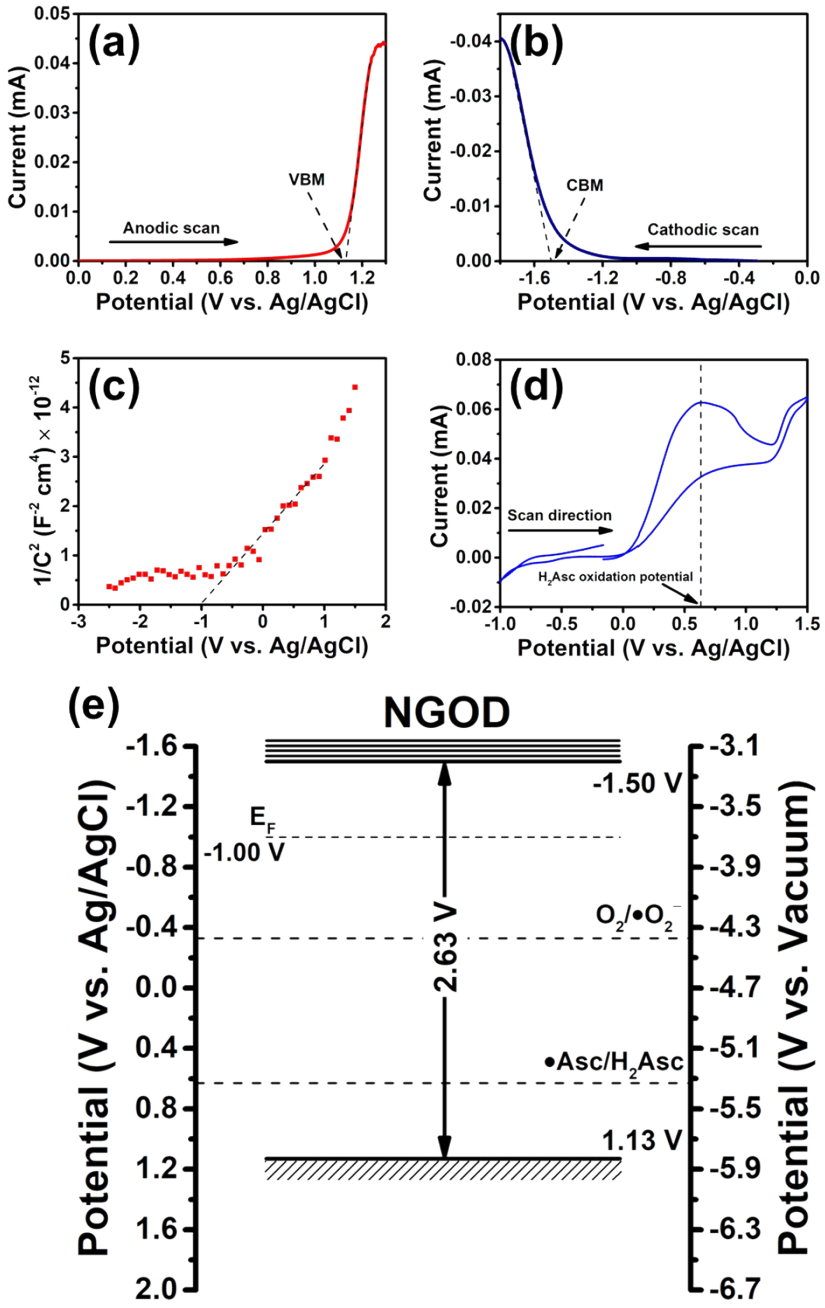

Fig. S10. Determining electronic band levels of NGODs: (a) anodic scanning to determine VBM at 0.5 mV s^{-1}; (b) cathodic scaning to determine CBM at 0.5 mV s^{-1}; (c) variations in capacitance (C) of NGOD electrode under applied potential in 0.1 M HNO_3 (which presented as the Mott-Schottky relationship and where capacitance was determined by electrochemical impedance spectroscopy and the Fermi level of NGODs was determined from the intercept of the extrapolated straight line on the abscissa); (d) cyclic voltammogram of 500 μM H_2Asc in 0.1 M HNO_3 at a scanning rate of 10 mV s^{-1}; (e) schematic energy level diagrams of NGODs compared with potentials for O_2 reduction and H_2Asc oxidation.

9. Determination of cell death mechanisms by Annexin V/PI assay

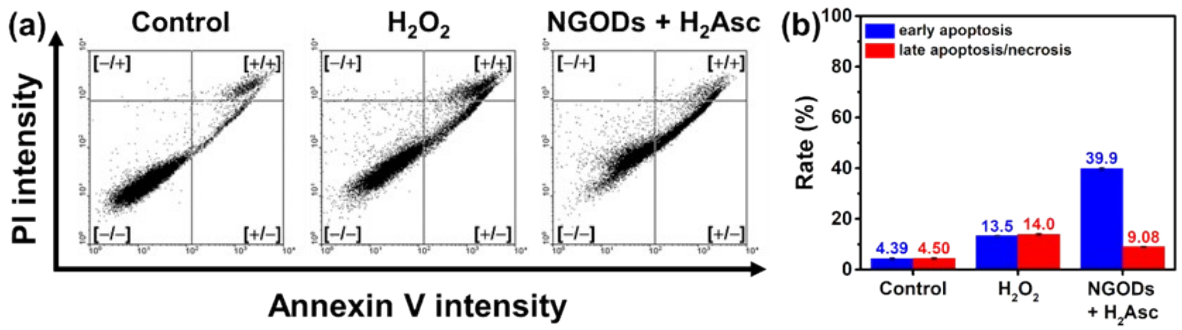

Fig. S11 Determining the cell death mechanisms triggered by NGOD-enhanced H_2Asc therapy using Annexin V/PI assay: (a) Cell populations in the early apoptotic and necrotic/late apoptotic stages were analyzed using Annexin V/PI assays. The distribution of cells in the control, positive control (100 μM H_2O_2), and NGOD-enhanced H_2Asc therapy-treated samples is shown on a plot of Annexin V against PI. (b) The ratios of early apoptotic and necrotic/late apoptotic populations after 24 h treatment are presented.

10. Determination of mitochondrial damage by TMRE assay

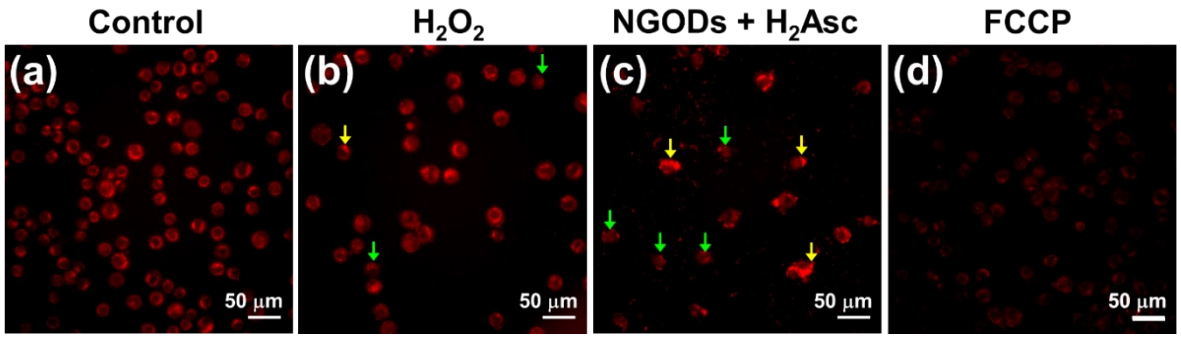

Fig. S12 Mitochondrial damage induced by NGOD-enhanced H_2Asc therapy was assessed using the tetramethylrhodamine ethyl ester (TMRE) assay. Representative TMRE fluorescence images of (a) untreated cells, (b) cells treated with 100 μM H_2O_2, (c) cells treated with NGOD-enhanced H_2Asc therapy (10 μg mL^{-1} NGODs with 200 μM H_2Asc), and (d) cells treated with 200 μM carbonyl cyanide 4-(trifluoromethoxy) phenylhydrazone (FCCP), an ionophore uncoupler of oxidative phosphorylation, as a positive control, are shown.